Carbohydrate Research, 61 (1978) 7–25

THE DOUBLE-HELICAL MOLECULAR STRUCTURE OF CRYSTALLINE B-AMYLOSE*†

HSIEN-CHIH HAROLD WU AND ANATOLE SARKO‡

Department of Chemistry, SUNY College of Environmental Science & Forestry, Syracuse, New York 13210 (U.S.A.)

(Received June 6th, 1977; accepted for publication in revised form, November 2nd, 1977)

ABSTRACT

The crystal structure of the B-polymorph of amylose appears to be based on double-stranded helices. The individual strands are in a right-handed six-fold helical conformation repeating in 20.8 Å and are wound parallel around each other. The steric disposition of O-6 is *gt*. The double helices pack in a hexagonal unit-cell ($a = b = 18.50$ Å, c (fiber repeat) $= 10.40$ Å, $\gamma = 120°$), with two helices (12 D-glucose residues) per cell. The helices are packed antiparallel and leave an open channel within a hexagonal array that is filled with water molecules. The reliability of the structure analysis is indicated by $R = 0.22$. The structure of B-amylose is consistent with the diffraction diagrams of B-starches and accounts for the physical properties of such starches.

INTRODUCTION

The B-form of amylose, one of the crystalline polymorphs of the linear (1 → 4)-α-D-glucan of starch, gives an X-ray diffraction diagram identical with that obtained from native B-starches. The latter are commonly found in tuberous plants and appear to be different in crystal structure from the A-starches usually found in grains. A third polymorph, C-starch, is more rare and is found in some plant sources[1]. All three starch types are crystalline and yield distinctive X-ray diffraction diagrams. The crystallinity of starches is generally understood to be due to the linear amylose, although some varieties of starch containing no amylose are also crystalline. In such cases, the crystallinity is due to the linear branches of amylopectin, the major component of almost all starches.

Despite the fact that the first published X-ray diffraction diagrams of starch were obtained in the 1930's, attempts to gain an understanding of the crystalline structure of starch have not been successful. For example, in 1944, Rundle, Daasch,

---

*Dedicated to Professor Dexter French on the occasion of his 60th birthday.
†Part VIII in the series "Packing Analysis of Carbohydrates and Polysaccharides".
‡To whom correspondence should be addressed.

and French[2] indexed a powder pattern of B-starch having an orthorhombic unit cell with parameters $a = 16.0$ Å, $b = 9.1$ Å, and $c = 10.6$ Å. They proposed a structure based on a two-glucose residue repeat along the chain axis. We now know that such a structure is stereochemically not possible. Similarly, the unit cell $a = 9.0$ Å, b (fiber repeat) $= 10.6$ Å, and $c = 15.6$ Å, proposed by Kreger[3] in 1951 on the basis of a pseudo-fiber diagram obtained from a single starch-granule, was thought to contain helical chains having a conformation of three residues per turn, and these are also improbable on stereochemical grounds. Later, in 1965, Schieltz[4] proposed a monoclinic unit cell having parameters $a = 12.0$ Å, $b = 16.25$ Å, $c = 10.48$ Å and $\gamma = 96.5°$. Again, although the chain structure was not specified, this unit cell is inconsistent with fiber X-ray data and cannot accommodate reasonable chain models.

In later work from this laboratory[5], based on well-oriented fiber X-ray data, a unit cell essentially double that of the Rundle–Daasch–French cell ($a = 16.0$ Å, $b = 18.2$ Å, c (fiber repeat) $= 10.40$ Å) was found to fit all of the diffraction spacings. Isolated-chain conformational analysis suggested six-fold helices, either 6_1 or 6_5, with water molecules intercalated between turns of the helix, as the most probable models for this fiber repeat. Subsequently, a hexagonal cell having sides $a = b = 18.33$ Å and $c = 10.41$ Å was also found to fit the diffraction data, but a packing analysis indicated that 6_1 or 6_5 helices, although possible, would pack very tightly and with distortions into this cell[6]. Nonetheless, the structure of B-amylose was considered at that time to be based on single, six-fold helices, although not quite like the model proposed by Blackwell *et al.*[5].

In follow-up work it became clear that none of the proposed single six-fold helices would satisfy the observed X-ray intensity distribution. It was not until the suggestion was made by Kainuma and French[7] in 1972, that the structure of B-starch could be double helical, that we realized such structures represented the more probable models for B-amylose. As we show here, the evidence for double-helical structure is now convincing and it is quite unlikely that the structure of B-starch could be based on single six-fold helices. In that respect, we now consider our earlier proposals for single helices to be much less likely.

In retrospect, it is clear why it has taken so long to understand the crystal structures of B-amylose and B-starch. In the first place, the preparation of suitable fiber specimens is difficult. More important, however, enormous amounts of computer time were needed to evaluate all of the models. We estimate that since the proposing of the correct hexagonal unit-cell in 1973, approximately 300 hours of computer time (CDC-3200) have been spent on the B-amylose structure, a figure that does not include the time spent in developing the structure-refinement methods employed in this study. It is obvious that a comparable structure-analysis could not have been accomplished without a computer.

EXPERIMENTAL

Fiber specimens for X-ray diffraction were prepared as previously described, by

solid-state deacetylation of crystalline fibers of amylose triacetate[5,8–10]. X-ray diffraction diagrams were recorded at each stage of conversion of the amylose triacetate into B-amylose, in order to observe any possible intermediate crystal-structures.

Immediately after deacetylation (with 0.2M potassium hydroxide, 75% ethanol), the fibers gave typical KOH-amylose diffraction patterns as described by Senti and Witnauer[9,10]. The conversion of the alkali amylose into well-oriented fibers of B-amylose then proceeded in three stages. First, the fibers were exposed to 80% relative humidity (r.h.) at room temperature for 3 days. The reflections appearing in the X-ray diagram taken after this stage (compare Table I) indicated that the sample was being converted into a mixture of B- and A-amyloses and was not going through a V-amylose stage as we had previously suspected[5]. In the second stage, the fibers were further crystallized by keeping them for 3 days in 100% r.h. at room temperature. The fibers were quite fragile at this stage and the characteristic 16-Å equatorial reflection of B-amylose was already present in their diffractograms. In the third step, the fibers were further annealed by heating them in water for one h at 90°.

The fibers of B-amylose obtained in this way gave diffraction diagrams of the same quality as previously published by us[5]. Only a sixth-order meridional reflection (d = 1.73 Å) appeared to be present in the diagram.

When a freshly prepared fiber of B-amylose was kept in 100% r.h. for two or more weeks at 90°, its diffraction diagram indicated the presence of a mixture of B- and A-amyloses[11]. Such a mixed diagram may be identical with the C-amylose patterns described by other workers[1,12].

X-Ray diffraction patterns were recorded on three-film packs of Ilford Type G Industrial X-ray film, using a Searle toroidal focusing camera and nickel-filtered Cu K_α radiation. During exposure, the fibers were kept in an atmosphere of 98% r.h. by means of a humidified stream of helium. The diffraction patterns intended for

TABLE I

THE d-SPACINGS EXHIBITED BY A B-AMYLOSE FIBER IMMEDIATELY AFTER CONVERSION FROM KOH–AMYLOSE[a]

Reflection (first number indicates layer line)	d-*Spacing (Å)*	*Relative intensity*[b]	*Source of reflection*[11]
0-1	5.92	W	A
0-2	5.39	M	B
0-3	4.96	W	A
1-1	5.88	W	A
1-2	5.38	M	B
1-3	4.03	W	B
2-1	3.80	W	A or B

[a]Fiber repeat = 10.7 Å. [b]M = moderate, W = weak.

d-spacing measurements were calibrated with sodium fluoride powder as an internal standard.

The relative intensity along each layer-line was traced by using a Joyce–Loebl automatic recording microdensitometer. Areas under the trace corresponding to individual reflections were determined by computer-assisted, least-squares resolution of the digitized intensity-envelope[13]. The areas were taken as a measure of the uncorrected relative intensity. Corrections were applied for polarization and Lorentz factor[14], variation in the spot-to-sample distance, spreading of the diffraction arc[14], and scanning direction other than normal to the diffraction arc. Relative observed structure-amplitudes were obtained by taking the square root of the relative intensities thus corrected. The intensity measurements were made on at least two sets of diagrams. The intensities of unobserved reflections were arbitrarily given a value of one-half of the minimum resolvable intensity in the corresponding region of the diffraction angle.

The density of the fiber, measured by flotation in a mixture of 1,4-dioxane–chloroform, was 1.45 g/cm^3. The water content of the fiber, calculated from elemental analysis (Galbraith Laboratories, Knoxville, Tenn.), was 5% for a fiber stored in vacuum, 10% for a fiber stored at room humidity, and 27% for a fiber exposed to 98% r.h. for 24 h.

RESULTS OF THE CRYSTAL-STRUCTURE ANALYSIS

The unit cell. — The *d*-spacings of a total of 27 observed reflections were measured. All reflections could be indexed with a hexagonal unit-cell $a = b = 18.50 \pm 0.10$ Å, c (fiber repeat) $= 10.40 \pm 0.04$, $\gamma = 120°$. The match of observed and

TABLE II

OBSERVED AND CALCULATED *d*-SPACINGS FOR B-AMYLOSE

hkl	d*(obs.)*, Å	d*(calc.)*, Å	hkl	d*(obs.)*, Å	d*(calc.)*, Å
100	16.14	16.02	121	5.27	5.23
110	9.06	9.25	031	4.70	4.75
200	7.97	8.01	131	4.07	4.09
120	6.00	6.05	041	3.76	3.74
300	5.34	5.34	231	3.43	3.46
220	4.59	4.62	241	2.92	2.91
400	4.00	4.01	112	4.56	4.53
320	3.66	3.67	032	3.75	3.73
140	3.47	3.49	222	3.43	3.45
420	3.00	3.03	042	3.18	3.17
060	2.67	2.67	142	2.91	2.90
250	2.58	2.57	123	3.03	3.01
011	8.77	8.72	043	2.63	2.63
021	6.34	6.35			

calculated *d*-spacings is shown in Table II. All of the diffraction lines found in powder patterns of B-starch can be indexed with this cell.

Some of the unit cells previously proposed on the basis of powder patterns, such as the Schieltz monoclinic cell[4], could not index all of the observed reflections. On the other hand, the Blackwell–Sarko–Marchessault orthorhombic cell[5], the Zugenmaier–Sarko orthorhombic cell[6] and the Zugenmaier–Sarko hexagonal cell[6], all proposed on the basis of fiber diagrams, could index all of the reflections reasonably well.

The measured fiber-density dictates that a maximum of 16 D-glucose residues can occupy this cell when the water content is at its minimum, namely 5%. Conversely, for the maximum water content—27%—the number of D-glucose residues is 12. The latter figure is the more reasonable of the two in view of the facile dehydration–rehydration of the sample and the fact that the diffraction intensities change with the water content of the sample. (The most prominent intensity change is seen in the 16-Å equatorial reflection, thus it is strong in an evacuated sample and weak in a fully hydrated one). At the same time, the unit-cell parameters do not change with the water content of the sample.

Because of the presence of the 16-Å equatorial reflection in the diffractogram, the two-chain orthorhombic unit cells[5,6] can be ruled out. (In these unit cells, the 16 Å reflection would be due to the *100* or *010* planes, which could not cause observable diffraction in a unit cell containing chains at its corners and in its center). In the hexagonal cell, the only reasonable arrangement of the 12 residues is in two helices, one located at $x = 2/3$, $y = 1/3$ and the other at $x = 1/3$, $y = 2/3$, with each helix containing six D-glucose residues. As shown later, the helices are double-stranded.

Stereochemical analysis. — Helix conformation. The presence of the sixth-order meridional is consistent with either a six-fold single helix with an axial rise per residue $h = 1.733$ Å, or a parallel, double-stranded helix with $h = 3.466$ Å and in which the two strands are exactly 180° out of phase in the *a–b* plane. For the latter model, a third-order meridional could be present. Antiparallel as well as any other parallel double helices having $h = 3.466$ Å are improbable because the *c* repeat of such structures would be 20.8 Å and layer lines consistent with this repeat should be present in the diffractogram.

The conformational probability of single 6_1 and 6_5 helices has previously been well documented[5,6]. Following the procedure of Bluhm and Sarko[15], we calculated conformational energy-maps for parallel double-stranded helices having bridge angles ranging from 105° to 120° and with different O-6 rotational positions. A representative such map, calculated with the bridge angle $\tau = 115°$ and O-6 in the *tg* position, is shown in Fig. 1. It can be seen that both left- and right-handed helices are probable, with the right-handed helix favored over the left-handed. The same calculations performed for antiparallel double helices showed that such helices were not likely because of short, interstrand contacts.

Chain packing. The unit-cell packing of all probable single and parallel-stranded, double-helical models was evaluated next, by using procedures previously

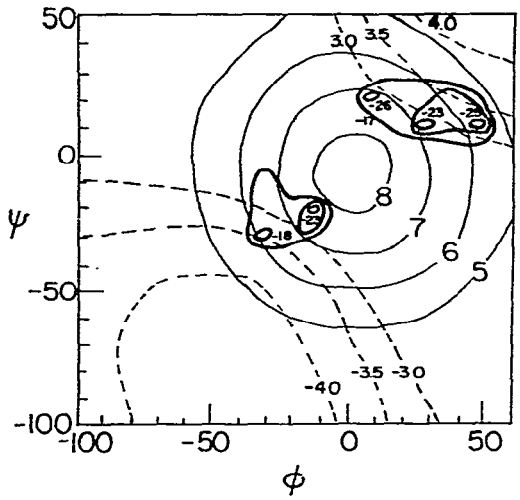

Fig. 1. Conformational-energy map for double parallel-stranded amylose helices having a bridge angle $\tau = 115°$. The energy contours are in kcal/mol; the thin, solid lines denote constant n (= number of residues/turn); the dashed lines denote constant h (= axial rise/residue in Å). Negative h indicates left-handed helices. For conventions and method of calculation, see Ref. 15.

described[16]. Essentially, the search for the optimal packing of the chains was performed by attempting to minimize the function:

$$Y = \sum_{i=1}^{l} \left(\frac{r_i - r_{0_i}}{SD_i^r}\right)^2 + \sum_{i=1}^{m} \left(\frac{\theta_i - \theta_{0_i}}{SD_i^\theta}\right)^2 + \sum_{i=1}^{n} \left(\frac{\phi_i - \phi_{0_i}}{SD_i^\phi}\right)^2 +$$

$$+ \frac{1}{W^2} \sum_{\substack{i=1 \\ j=1}}^{N} w_{ij}(d_{ij} - d_{0_{ij}})^2 \qquad (1),$$

where r_i, θ_i and ϕ_i are, respectively, the bond lengths, bond angles, and conformational angles for the l, m, and n corresponding variables in the monomer residue, while r_{0_i}, θ_{0_i}, ϕ_{0_i} and SD_i^r, SD_i^θ, SD_i^ϕ are their standard values and standard deviations, respectively. The first three terms of this function represent components of conformational energy, in particular, the bond-length, bond-angle, and conformational-angle strains occurring during the adjustment of these variables. The remaining term approximates the nonbonded repulsion, with d_{ij} the distance between the nonbonded atoms i and j, $d_{0_{ij}}$ the corresponding equilibrium distance, w_{ij} the weight assigned to a given contact in the summation, and W the weight of the nonbonded-contact term in the entire function Y. All nonbonded contacts, namely those within the chain, as well as those between the strands of an individual double-helix and those between different double helices, are included in the last term of Eq. *1*. This term thus represents both conformational and packing nonbonded repulsion-energy. As was done before, the values for r_{0_i}, θ_{0_i}, and ϕ_{0_i} were taken from the Arnott-Scott compilation of average stereochemical data for sugars[17], and the values of $d_{0_{ij}}$ and w_{ij} came from our own

TABLE III

PACKING OF PARALLEL-STRANDED DOUBLE HELICES AND SIXFOLD SINGLE HELICES (V.B. = 4.25 Å)

Helix type	*Chirality*	*O-6*[a] *(deg.)*	*Bridge angle (deg.)*	*P.E.*[b] *(pack./ conf.)*	*Helix positions*[c]			*Hydrogen bonds and lengths, Å*[d]		*Short packing-contacts*
					Helix 1 rotation (deg.)	*Helix 2 rotation (deg.)*	*Helix 2 translation (Å)*			
Double, parallel packed	Right-handed	gt (59)	106	30/29	0.2	— 2.7	0.16	$O\text{-}3_3\text{-}O\text{-}6_4$	2.61	None
								$O\text{-}2_3\text{-}O\text{-}6_8$	2.60	
								$O\text{-}6_5\text{-}O\text{-}2_{12}$	2.65	
Double, parallel packed	Left-handed	gg (−73)	105	34/26	−5.1	2.3	−4.01	$O\text{-}6_3\text{-}O\text{-}2_4$	2.68	None
								$O\text{-}6_1\text{-}O\text{-}3_{10}$	2.98	
								$O\text{-}3_1\text{-}O\text{-}3_{11}$	2.91	
Double, anti-parallel packed	Right-handed	gt (59)	106	26/29	0.3	9.5	0.90	$O\text{-}3_3\text{-}O\text{-}6_4$	2.64	None
								$O\text{-}6_5\text{-}O\text{-}6_{10}$	2.72	
Double, anti-parallel packed	Left-handed	gg (−73)	105	25/26	−3.2	4.2	−2.76	$O\text{-}6_3\text{-}O\text{-}2_4$	2.68	None
								$O\text{-}3_4\text{-}O\text{-}3_{11}$	2.66	
Single parallel packed	Right-handed	gt (63)	118	198/17	0.3	8.0	0.08	None		24 contacts
Single parallel packed	Left-handed	gt (69)	118	163/17	50.5	−37.1	−2.65	$O\text{-}5_2\text{-}O\text{-}6_{12}$	2.84	18 contacts
								$O\text{-}2_2\text{-}O\text{-}6_{13}$	2.90	
Single anti-parallel packed	Right-handed	gt (61)	118	186/17	0.2	−9.9	0.17	None		30 contacts
Single anti-parallel packed	Left-handed	gt (63)	117	122/19	72.9	−37.7	−2.36	None		13 contacts

[a] O-6 is at 0° when the bond sequence O-5–C-5–C-6–O-6 is *cis*. Rotation of C-6–O-6 is positive-clockwise looking from C-5 to C-6, and pure $gt = 60°$, $tg = 180°$, and $gg = -60°$. [b] P.E. is the packing energy, from the nonbonded term of Eq. *1*. The first number indicates inter-strand and inter-helix packing energy, while the second number indicates intra-chain, or conformational energy. For reasonable models, this packing energy should not exceed the higher 30's. [c] Helix 1 is at $\frac{2}{3}\,a, \frac{1}{3}\,b$ and helix 2 is at $\frac{1}{3}\,a, \frac{2}{3}\,b$. The 0° rotational position for both helices is such that the vector from the helix axis to O-4 of the first residue is parallel to the *b* axis and extends toward $-b$. Positive rotation is clockwise looking down the *c* axis. Translation of helix 2 is relative to helix 1 along *c*. [d] Subscripts indicate residue numbers: 1–3 are in chain 1 of helix 1, 4–6 are in chain 2 of helix 1, 7–9 are in chain 1 of helix 2, and 10–12 are in chain 2 of helix 2.

TABLE IV

PACKING OF HELICES HAVING DIFFERENT VIRTUAL BOND-LENGTHS

Helix type	*Chirality*	*VB (Å)*	*Bridge angle (deg.)*	*P.E.[a] (pack./conf.)*	*Short packing-*
Double,	Right-handed	4.25	106	26/29	None
antiparallel packed		4.45	116	75/21	6 contacts
O-6 *gt*		4.60	118	99/17	9 contacts
Single parallel	Left-handed	4.00	108	60/16[b]	9 contacts[b]
packed[b]		4.25	118	163/17	18 contacts
Single,	Left-handed	4.00	108	55/16[b]	9 contacts[b]
antiparallel packed[b]		4.25	117	122/19	13 contacts

[a]See Footnote *b* in Table III. [b]O-6 contacts are not included.

previous work[18]. The value for *W* was fixed at 0.5. The D-glucose residue was in the $^4C_1$ conformation.

For each helix that was investigated, both left- and right-handed conformations and parallel and antiparallel modes of packing needed to be tested. Each helix model was also constructed with several different lengths of the D-glucose residue, that is, with varying lengths of the virtual bond. (The virtual bond, or VB, is a vector connecting successive glycosidic oxygen atoms along the helix. Its length determines the maximum bridge-angle that can be reached in a given helix). The three primary rotational positions of O-6—*gt*, *gg*, and *tg*—constituted an additional starting variable. In all, a total of 40 models were investigated. The results of this packing analysis are illustrated in Tables III and IV. For simplicity, Table III shows the features and packing characteristics for one of each of the major helix models, with a fixed virtual bond-length of 4.25 Å, whereas Table IV shows a comparison with varying virtual bond-lengths.

It is clear from the results of Table III that neither the 6_1 nor the 6_5 single helix could be packed into this unit cell. At a virtual bond-length of 4.25 Å, the diameter of the single helix is nearly at its lowest for reasonable stereochemical features of the D-glucose residue, and yet numerous short contacts exist between the helices. Increasing the length of the virtual bond only increases the helix diameter, thus making the packing worse. An attempt was made to construct single helices based on a residue having a virtual bond of 4.0 Å, even though such short residues have not been observed in crystal structures of sugars. The resulting helices, although narrower in diameter, still did not pack without short contacts (compare Table IV). These results confirmed our previous findings with regard to the hexagonal cell[6].

On the other hand, the parallel-stranded double helices having a virtual bond-length of 4.25 Å packed readily into the unit cell, regardless of helix chirality or the packing polarity. In almost all cases, all three O-6 positions were possible, with the exception of the right-handed, antiparallel packed helices with O-6 *gg*, which showed unacceptable short contacts. The only unusual characteristic of these double helices

was a lower bridge angle, 105 ± 1°, than is usually observed in crystal structures of di- or higher saccharides. Most other stereochemical features were within one standard deviation of the average values[17]. Increasing the length of the virtual bond allowed an increase in the bridge angle, but this was accompanied by an increase in the repulsive packing-energy and an appearance of unacceptable short contacts. The extent of the increase in packing energy with increasing virtual bond-lengths is illustrated in Table IV. Similarly, the bridge angle could be forced to larger values for any virtual bond-length at the expense of other bond angles; however, subsequent X-ray refinement showed these models to be unacceptable.

It is thus clear that right-handed and left-handed, parallel-stranded double helices in either parallel or antiparallel packing are the favored models on stereochemical grounds. It also appears that the chains increase their packing stability at the expense of lowering the bridge angle, that is, at the expense of lowered conformational stability.

X-Ray refinement. — Despite the indications from stereochemical analysis that the double helix was the only probable helix type for B-amylose, the most probable model from among several could not be picked. It was, therefore, necessary to refine all probable models. With two packing polarities, the chirality of the helices, and three primary rotational positions for O-6 as variables, a total of 12 models had to be tested. The problem was further complicated by the fact that the water contained in the unit cell had now to be included. Because of the large number of tests and in view of the reliability of the equatorial intensity-data, it was decided to make a preliminary screening of all models by two-dimensional X-ray refinement. It was hoped that the positions of water molecules could be located in projection by this method.

Two-dimensional refinement and water positions. As the packing analysis suggested, the majority of the water molecules appeared to be located in the fairly large empty space at the corners of the unit cell. The tight packing of the individual strands of the double helix, and the close fit of helices in the unit cell, made it impossible to fit any water molecules either inside the helices or between them. Consequently, in the fully hydrated sample (containing 27% of water) a maximum of 42 water molecules, or approximately 3.5 water molecules per sugar residue, could be located in that space. The simplest way to treat such a large amount of water in this nearly cylindrical channel was to imagine it to be arranged in the form of a cylinder of some average radius. Therefore, all models were tested, in projection, with a column of water at the origin of the unit cell, and with the number of water molecules in the column and the radius of the column as systematically variable parameters. The amylose helix was in each case the corresponding best stereochemical model and it was left invariant in the process. The goodness criterion was the usual crystallographic reliability index

$$R = \frac{\sum| \, |F_o| - |F_c| \, |}{\sum |F_o|},$$

TABLE V

TWO-DIMENSIONAL *R*-VALUES FOR RIGHT-HANDED DOUBLE HELICES AND TWO SINGLE HELICES AS A FUNCTION OF NUMBER AND ARRANGEMENT OF WATER MOLECULES

No. of H_2O per residue	*Radius of water column (Å)*	R-*Value*	
		VB = 4.25 Å	*VB = 4.45 Å*
Double right-handed helix (antiparallel packed, O-6gt)			
2.5	2.0	0.560	0.531
	2.5	0.287	0.301
	3.0	0.165	0.181
	3.5	0.325	0.360
3.0	2.0	0.625	0.604
	2.5	0.319	0.339
	3.0	0.156	0.196
	3.5	0.327	0.395
3.5	2.0	0.657	0.612
	2.5	0.361	0.361
	3.0	0.208	0.257
	3.5	0.334	0.443
Single helix (left-handed, parallel packed, O-6gt)			
		(VB = 4.0 Å)	(VB = 4.25 Å)
3.0	2.0	0.72	
	2.5	0.58	0.55
	3.0	0.61	0.65
	3.5	0.75	
Single helix (left-handed, antiparallel packed, O-6gt)			
3.0	2.0	0.67	
	2.5	0.58	0.55
	3.0	0.51	0.54
	3.5	0.63	

where F_c and F_0 are the calculated and observed structure-amplitudes, respectively. Included in this test, just for comparison, were single helices having virtual bond-lengths at 4.0 and 4.25 Å, even though both had been ruled out by stereochemical analysis.

The results of this testing are shown in Table V, for the double right-handed helix (O-6 *gt*) in antiparallel packing, which turned out to be the best of the double-stranded helices, and for left-handed single helices in parallel and antiparallel packing. It is clear that the best agreement is obtained with three water molecules per residue (total 36 H_2O) arranged in a column with a 3-Å radius. The calculated density with this amount of water in the unit cell is 1.40 g/cm^3, which is in fair agreement with the measured density of 1.45 g/cm^3. It is also evident that a D-glucose residue having a virtual bond-length of 4.25 Å is again a better choice than a longer residue. All of the other double-helical models gave the same results as regards the water column, but their *R* values were considerably higher than those obtained with the best model.

TABLE VI

TWO-DIMENSIONAL R-VALUES OF DOUBLE-HELICAL MODELS (CONTAINING 36 H_2O) AFTER REFINEMENT (v_B = 4.25 Å)

Model	*O-6*[a] *(deg.)*	*Bridge angle (deg.)*	*Helix rotations*[b]		*R*
			Helix 1 (deg.)	*Helix 2 (deg.)*	
Double right-handed helix in antiparallel packing	*gt* (77)	106	—3.8	3.8	0.065
	tg (160)	104	—7.1	4.2	0.163
	gg (—53)	104	—8.9	19.2	0.116
Double right-handed helix in parallel packing	*gt* (63)	106	—5.0	—2.7	0.135
	tg (179)	106	—5.6	—7.2	0.152
	gg (—63)	105	—8.4	3.9	0.191

[a]See Footnote *a* in Table III. [b]See Footnote *c* in Table III.

Nevertheless, all models were subjected to two-dimensional refinement, with the following model variables: independent rotation of the two double helices about their helix axes, rotation of the sugar residue about the virtual bond, the length of the virtual bond (in discrete steps), rotation of O-6, and the rotation of the water column about the *c* axis of the unit cell. Because the single helices gave very poor *R*-values, they were not tested any further.

Again, the best results were obtained with the right-handed, double parallel-stranded helix in antiparallel packing, with O-6 *gt* and with a virtual bond-length of 4.25 Å. The results are shown in Table VI, with other O-6 positions included for comparison. The next-best model, that of the same helix in parallel packing, is also shown. The rotational positions of the helices in both models can be seen to be quite close to the positions predicted by the packing analysis (compare Table III). The left-handed models would not refine without serious, interstrand short-contacts between C-6 and O-2 (2.48 Å) and were eliminated from further consideration at this point.

The effect on the *R*-value and the equatorial intensity-distribution of varying the virtual bond-length of the best model is shown in Table VII. It is clear that increasing the length of the virtual bond, accompanied by an increase in the bridge angle, results in a progressively poorer fit of calculated and observed intensities. It could be argued that a difference between *R*-values of, for example, 0.065 and 0.113 may only be marginally significant. However, the measured equatorial intensities for B-amylose are very reliable, and therefore the poor fit obtained with intensities

TABLE VII

COMPARISON OF OBSERVED AND CALCULATED EQUATORIAL STRUCTURE-AMPLITUDES FOR THE REFINED, DOUBLE RIGHT-HANDED, ANTIPARALLEL-PACKED HELIX MODELS (WITH 36 H_2O) AS A FUNCTION OF VIRTUAL BOND-LENGTH

hkl	F_o	F_c		
		V.B. = 4.25 Å	*V.B. = 4.45 Å*	*V.B. = 4.60 Å*
100	59	64	63	48
110	15	33	29	50
200	43	68	105	105
120	122	106	113	74
300	234	225	187	201
220, 130	252	252	250	250
400	80	81	83	82
320	81	78	81	78
140	147	147	141	148
050, 330, 420, 150	172	172	152	171
430, 060	177	157	177	179
250, 160	127	127	126	123
	R =	0.065	0.113	0.137

calculated for all virtual bond-lengths larger than 4.25 Å strongly argues against such models. Similar deterioration in the fit was observed when the bridge angle for the VB = 4.25 Å model was forced to values larger than 105° at the expense of other bond angles in the D-glucose ring. Thus, both stereochemical and X-ray intensity-analyses point toward a double helix for B-amylose that has a lower bridge-angle than may be expected in single-helical conformations of the same glucan.

Final three-dimensional refinement. In view of only 34 available intensities, the final refinement of a structure containing 36 water molecules could not be carried out with all water molecules being kept independent. Instead, a stratagem was devised in which the water column was divided into six planes, each containing six water molecules equally spaced along a circle having a 3-Å radius. The planes were equally spaced along the *c* repeat of the unit cell. The approximate translational positions of the second helix (at 1/3*a*, 2/3*b*) and the water column along the *c* axis were then found by refining in two stages against three-dimensional intensity data. In the first stage, five variable parameters were refined: two independent helix-rotations, rotation of the sugar residue about the virtual bond, rotation of O-6, and translation of the second helix. The translational position of the first helix (at 2/3*a*, 1/3*b*) was fixed at 0*c*. In the second stage, the positions of the six planes of water molecules were refined, with 18 variables (3 *x*,*y*,*z* coordinates for each plane). In the final run, all 23 variables were

TABLE VIII

CHARACTERISTICS OF THE FINAL RIGHT-HANDED, ANTIPARALLEL-PACKED, DOUBLE-HELIX STRUCTURE, AFTER THREE-DIMENSIONAL X-RAY REFINEMENT

O-6[a]	*Bridge angle*	VB (Å)	*Helix positions*[b]			*Hydrogen bonds and lengths*[c] *(Å)*		*Short packing-contacts*
			Helix 1 rotation	*Helix 2 rotation*	*Helix 2 translation*			
gt (67°)	105°	4.25	—13.8°	6.2°	—1.12 Å	$O\text{-}3_3$–$O\text{-}6_4$	2.68	None
						$O\text{-}2_2$–$O\text{-}6_4$	2.95	
						$O\text{-}2_1$–$O\text{-}5_8$	2.59	
						$O\text{-}6_4$–$O\text{-}2_{11}$	2.83	

[a]See Footnote *a* in Table III. [b]See Footnote *c* in Table III. [c]See Footnote *d* in Table III.

TABLE IX

OBSERVED AND CALCULATED STRUCTURE-AMPLITUDES FOR THE BEST MODEL OF B-AMYLOSE

hkl	$F_{obs.}$	$F_{calc.}$	hkl	$F_{obs.}$	$F_{calc.}$
100	59	73	041	143	88
110	15	27	141	30	41
200	43	74	231	170	91
120	122	107	051, 331	191	132
300	234	244	241		
220	252	249	012	20	26
130			112	61	43
400	80	81	022	25	148
320	81	104	122	225	162
140	147	143	032		
050, 330	172	161	222	114	129
420, 150			132		
060	177	150	042	80	93
430			322	230	202
250	127	127	142		
160			103	30	30
011	25	33	113	33	32
111	77	177	023	35	59
021			123	116	91
121	190	192	033	40	39
031	52	91	223, 043	230	194
221	220	212	133, 233		
131					

refined simultaneously. This process was repeated for several different combinations of initial values for the variable parameters, particularly helix rotations. The refinement was not carried any further in the sense that no additional structural parameters of the molecule, such as bond and conformation angles, were allowed to become

TABLE X

CARTESIAN ATOMIC COORDINATES OF ONE RESIDUE OF EACH CHAIN

Atom	*X, Å*	*Y, Å*	*Z, Å*
1. *Helix at* (2/3a, 1/3b) *Chain 1*			
C-1	13.856	—1.800	3.119
C-2	14.424	—1.566	1.712
C-3	13.302	—1.482	0.683
C-4	12.389	—2.690	0.821
C-5	11.905	—2.885	2.266
C-6	11.155	—4.182	2.472
O-1	13.043	—0.683	3.467
O-2	15.223	—0.386	1.697
O-3	13.906	—1.493	—0.609
O-4	11.271	—2.387	0.0
O-5	13.063	—2.963	3.110
O-6	10.619	—4.305	3.781
H-1	14.639	—1.304	3.811
H-2	15.037	—2.381	1.465
H-3	12.753	—0.596	0.818
H-4	12.873	—3.556	0.476
H-5	11.305	—2.074	2.555
H-6a	11.795	—4.992	2.278
H-6b	10.361	—4.217	1.786
2. Chain 2			
C-1	7.506	1.800	3.119
C-2	6.838	1.566	1.712
C-3	8.060	1.482	0.683
C-4	8.973	2.690	0.821
C-5	9.457	2.885	2.266
C-6	10.207	4.182	2.472
O-1	8.319	0.683	3.467
O-2	6.139	0.386	1.697
O-3	7.456	1.493	—0.609
O-4	10.091	2.387	0.0
O-5	8.299	2.963	3.110
O-6	10.743	4.305	3.781
H-1	6.723	1.904	3.811
H-2	6.325	2.381	1.465
H-3	8.609	0.596	0.818
H-4	8.489	3.556	0.476
H-5	10.057	2.074	2.555
H-6a	8.567	4.832	2.278
H-6b	11.001	4.217	1.786
3. Helix at (*1*/3a, *2*/3b) *Chain 1*			
C-1	2.436	7.040	6.161
C-2	1.841	7.196	7.568
C-3	2.942	7.430	8.597
C-4	4.009	6.355	8.459
C-5	4.515	6.227	7.014
C-6	5.432	5.042	6.808
O-1	3.091	8.256	5.813

Table X *(continued)*

Atom	*X, Å*	*Y, Å*	*Z, Å*
O-2	0.891	8.258	7.583
O-3	2.345	7.337	9.889
O-4	5.077	6.805	9.280
O-5	3.378	5.994	6.170
O-6	5.980	4.992	5.499
H-1	1.674	6.832	5.469
H-2	1.343	6.305	7.815
H-3	3.367	8.381	8.462
H-4	3.646	5.432	8.804
H-5	5.001	7.111	6.725
H-6a	4.907	4.154	7.002
H-6b	6.224	5.114	7.494
4. Chain 2			
C-1	8.245	11.460	6.161
C-2	8.840	11.304	7.568
C-3	7.739	11.070	8.597
C-4	6.672	12.145	8.459
C-5	6.166	12.273	7.014
C-6	5.249	13.458	6.808
O-1	7.590	10.244	5.813
O-2	9.790	10.242	7.583
O-3	8.336	11.163	9.889
O-4	5.604	11.695	9.280
O-5	7.303	12.506	6.170
O-6	4.701	13.508	5.499
H-1	9.007	11.668	5.469
H-2	9.338	12.195	7.815
H-3	7.314	10.119	8.462
H-4	7.036	13.068	8.804
H-5	5.680	11.389	6.725
H-6a	5.774	14.346	7.002
H-6b	4.457	13.386	7.494

variables. It was felt that, in view of the somewhat indeterminate character of the 36 water molecules (which represent a sizable fraction of the contents of the unit cell), a detailed refinement of the polysaccharide molecule was not justified. Nevertheless, as the results presented in Tables VIII and IX show, the final structure shows no unreasonable features. The final R index of 0.224 indicates a high degree of reliability. The structure shows hydrogen bonds of reasonable length. The rotational positions of the helices and the translation of the second helix along its axis are in fairly good agreement with the corresponding values determined on the basis of packing (compare Table III), but are not in so good an agreement as had been obtained in the structure analysis of V-amylose[16]. This is not surprising, because the packing refinement was done without water and its minimum was quite broad, whereas the X-ray refinement was accomplished with water present in the structure. (The ranges of X-ray refined,

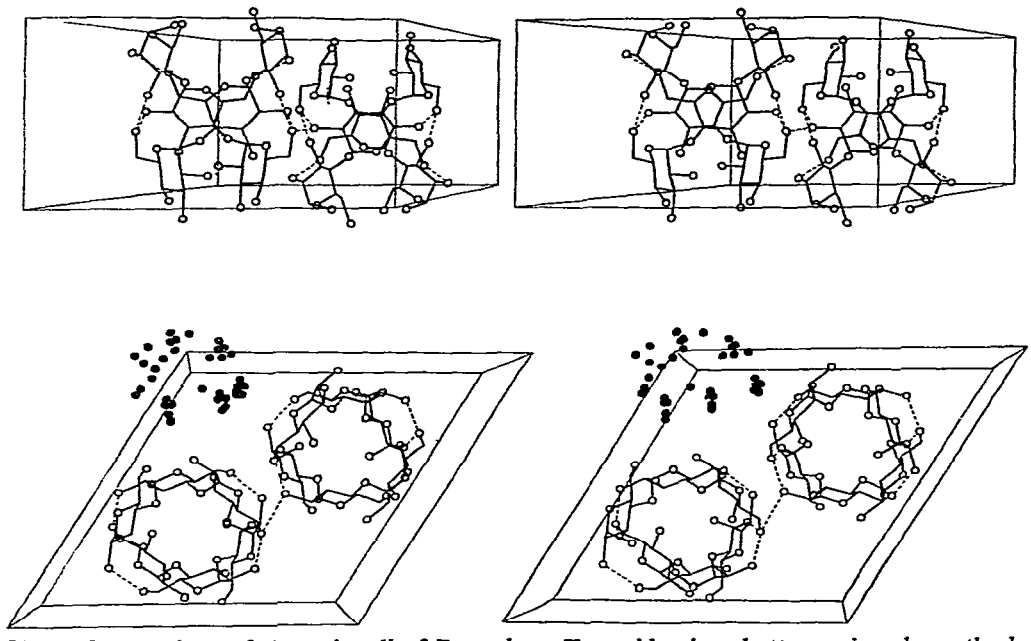

Fig. 2. Stereo views of the unit cell of B-amylose. Top: side view, bottom: view down the helix axis. Water positions are indicated in the lower view by dots. Hydrogen atoms are not shown. Hydrogen bonds are indicated by dashed lines.

helix rotations and translation were surprisingly small: less than one degree for rotation and approximately 0.2 Å for translation). There are no short contacts between the chains in the final structure. Finally, the calculated and observed structure-amplitudes are in very good agreement, with only a few higher-level reflections showing sizeable differences. This is particularly remarkable and shows that the liberties taken with the water column were not unreasonable. The atomic coordinates of the final structure are listed in Table X and a stereo view of the structure is shown in Fig. 2.

DISCUSSION

The probable double-helical structure of B-amylose is characterized by some surprising features, particularly the small bridge-angle and the hexagonal packing of double helices around a large cavity (compare Fig. 3). The fact that B-amylose appears to be double helical should not come as a surprise because, as discussed later, a double-helical structure is more in agreement with the physical properties of starch than any single-helical structure.

The rather small bridge angle of $\sim 105°$ appears to be a true structural feature and not an artifact of crystal-structure refinement. Both stereochemical and X-ray refinement point toward this angle; any attempt to increase it, either by lengthening the virtual bond or by distorting the sugar residue, immediately results in simultaneous

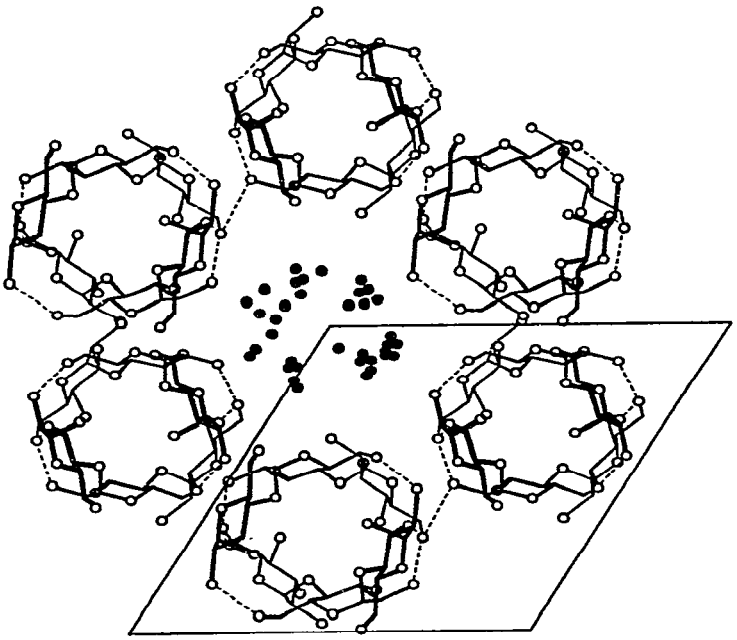

Fig. 3. Packing arrangement of double-helices of B-amylose.

increases in the packing energy and the *R*-value. In the type of refinement method used here, it would be impossible to hold the bridge angle at an improbable value. It thus appears that the bridge angle here is just another flexible parameter that adjusts itself in order to provide the molecule and the crystal structure with the highest possible stability. Such stability may be achieved by increasing the number or strength of hydrogen bonds, with a resultant lowering of the total energy by several kcal./mol.

Both the double-helical structure and the type of packing of B-amylose are consistent with the properties of granular starch. Even though the latter is crystalline, it is readily permeated by water, small organic molecules, and iodine. All of the latter can fit easily into the channel formed by the hexagons of double helices (compare Fig. 3), because the diameter of the channel is approximately the same as that of a double helix, of the order of 8 Å. The approximate volume of such a channel in one *c* repeat of the unit cell is larger than 500 $Å^3$, which is more than sufficient to accommodate 36 water molecules. (It should be understood that 36 water molecules constitute only the most probable figure. The actual number may be different by several molecules or may even be variable). The labile arrangement of water in that channel is also consistent with the relative ease with which both B-amylose and B-starch lose water on dehydration. This loss of water is reflected in the intensity of the *100* reflection which changes with the water content. (The increase in the intensity of the *100* reflection upon dehydration of a fully humidified sample is approximately 5-fold, which is exactly as predicted by structure-factor calculations).

Whether iodine actually enters this channel to give the intense blue color seen with starch is not known. The channel is certainly sufficiently large to accommodate iodine; on the other hand, much of the starch granule is non-crystalline and the polysaccharide in the amorphous regions could well complex with iodine to give the helical arrangement proposed by Rundle[19] and Zaslow and Miller[20].

Notwithstanding the ready accessibility of the crystalline portions of B-amylose to water, neither B-starch nor B-amylose are readily solubilized in water. Starch granules must be heated above 70° before they begin to dissolve, whereas pure B-amylose can only be solubilized by autoclaving. The difference in solubility behavior between starch and amylose resides in the high amylopectin content of the granule, as amylopectin is readily soluble in water. The resistance to dissolution is undoubtedly due to the extensive network of intra- and interhelical hydrogen bonds that stabilize the double-helical structure of crystalline amylose. In contrast, the less extensively hydrogen-bonded, single-helical structure of V-amylose[16,21] is readily dissolved in water.

Because the channel in the crystal structure of B-amylose is of approximately the same diameter as a double helix, it is also probable that partial occupancy of it by a double helix may occur under some circumstances. For example, granular starches may be eroded by dilute mineral acids over a period of weeks or months to give the "Nägeli amylodextrin", which, as Kainuma and French have shown, is much more crystalline and appears to have a low water content[7]. By the action of acid, the amorphous polysaccharide is slowly and randomly hydrolyzed, which permits an increase in the perfection of the crystalline regions. The increasing crystallinity may be accompanied by partial filling of the water channels with double helices, thus displacing the water. If this happens, the *100* reflection should weaken considerably in intensity or even disappear, and there is evidence of this happening in the Kainuma–French X-ray patterns.

Such an increase in packing density should be accompanied by an increase in the crystalline density (to a maximum of 1.57 g/ml) and a further resistance to water solubility. It is not known whether the former is true, but the latter has been observed.

The double-helical character of amylose is also consistent with the gelation behavior of starch. When hot aqueous solutions of either starch or amylose are cooled, strong gels form that display syneresis, become crystalline, and are thermally irreversible up to autoclaving temperatures. Their crystalline pattern is that of B-amylose. All of these properties are enhanced by increasing the content of amylose in the gel. This process is frequently troublesome in the starch industry and is known as "retrogradation". As Rees described it some years ago, the gelling of carrageenans is the result of double-helical "crosslinks" in the polysaccharide gel[22,23]. The same process may occur in starch gelling and retrogradation. The avoidance of retrogradation, then, may reside in avoiding the double-helical ordering of amylose.

ACKNOWLEDGMENT

This work was supported by National Science Foundation grant No. CHE7501560.

REFERENCES

1 C. STERLING, in J. A. RADLEY (Ed.), *Starch and its Derivatives*, 4th edn., Chapman and Hall, London, 1968, p. 152.
2 R. E. RUNDLE, L. DAASCH, AND D. FRENCH, *J. Am. Chem. Soc.*, 66 (1944) 130–134.
3 D. R. KREGER, *Biochim. Biophys. Acta*, 6 (1951) 406–425.
4 N. C. SCHIELTZ, *Quart. Colo. School Mines*, 60 (4) (1965) 55–58.
5 J. BLACKWELL, A. SARKO, AND R. H. MARCHESSAULT, *J. Mol. Biol.*, 42 (1969) 379–383.
6 P. ZUGENMAIER AND A. SARKO, *Biopolymers*, 12 (1973) 435–444.
7 K. KAINUMA AND D. FRENCH, *Biopolymers*, 11 (1972) 2241–2250.
8 A. SARKO, R. H. MARCHESSAULT, *J. Am. Chem. Soc.*, 89 (1967) 6454–6462.
9 F. R. SENTI AND L. P. WITNAUER, *J. Am. Chem. Soc.*, 68 (1946) 2407–2408.
10 F. R. SENTI AND L. P. WITNAUER, *J. Am. Chem. Soc.*, 70 (1948) 1438–1444.
11 H. C. H. WU AND A. SARKO, *Carbohydr. Res.*, 61 (1978) 27–40.
12 S. HIZUKI, *Agric. Biol. Chem.*, 25 (1961) 45–49.
13 R. D. B. FRASER AND E. SUZUKI, *Anal. Chem.*, 38 (1966) 1770–1773.
14 R. J. CELLA, B. LEE, AND R. E. HUGHES, *Acta Crystallogr. Sect. A*, 26 (1970) 118–124.
15 T. BLUHM AND A. SARKO, *Carbohydr. Res.*, 54 (1977) 125–138.
16 P. ZUGENMAIER AND A. SARKO, *Biopolymers*, 15 (1976) 2121–2136.
17 S. ARNOTT AND W. E. SCOTT, *J. Chem. Soc., Perkin Trans. 2*, (1972) 324–335.
18 P. ZUGENMAIER AND A. SARKO, *Acta Crystallogr. Sect. B*, 28 (1972) 3158–3166.
19 R. E. RUNDLE, *J. Am. Chem. Soc.*, 69 (1947) 1769–1772.
20 B. ZASLOW AND R. L. MILLER, *J. Am. Chem. Soc.*, 83 (1961) 4378–4381.
21 W. T. WINTER AND A. SARKO, *Biopolymers*, 13 (1974) 1447–1460.
22 D. A. REES, *Adv. Carbohydr. Chem. Biochem.*, 24 (1969) 267–332.
23 D. A. REES, *Biochem. J.*, 126 (1972) 257–273.